THE GLYCOSYLTRANSFERASE EOGT REGULATES ADROPIN EXPRESSION IN DECIDUALIZING HUMAN ENDOMETRIUM

Joanne Muter[1], Mohammad T Alam[1], Pavle Vrljicak[1,2], Flavio SV Barros[1], Peter T Ruane[3,4], Lauren J Ewington[1,2], John D Aplin[3,4], Melissa Westwood[3,4], and Jan J Brosens[1,2]

[1]Division of Biomedical Sciences, Clinical Science Research Laboratories, Warwick Medical School, University of Warwick, Coventry CV2 2DX, UK.

[2]Tommy's National Centre for Miscarriage Research, University Hospitals Coventry & Warwickshire, Coventry CV2 2DX, UK.

[3]Maternal and Fetal Health Research Centre, Division of Developmental Biology and Medicine, School of Medical Sciences, Faculty of Biology, Medicine and Health, University of Manchester, Manchester Academic Health Sciences Centre, St. Mary's Hospital, Manchester M13 9WL, UK.

[4]Maternal and Fetal Health Research Centre, St. Mary's Hospital, Central Manchester University Hospitals NHS Foundation Trust, Manchester Academic Health Sciences Centre, Manchester M13 9WL, UK.

Abbreviated Title: EOGT in the endometrium

Keywords: endometrium, decidualization, EOGT, adropin, O-GlcNAcylation, BMI

Corresponding Author and person to whom reprint requests should be addressed:

Joanne Muter, PhD, Division of Biomedical Sciences, Clinical Science Research Laboratories, Warwick Medical School, University of Warwick, Coventry CV2 2DX, UK, Tel: +44 2476968684; Email: j.muter@warwick.ac.uk

Disclosure Statement: I certify that neither I nor my co-authors have a conflict of interest as described above that is relevant to the subject matter or materials included in this Work.

Abstract

In pregnancy, resistance of endometrial decidual cells to stress signals is critical for the integrity of the feto-maternal interface and, by extension, survival of the conceptus. O-GlcNAcylation is an essential post-translational modification that links glucose sensing to cellular stress resistance. Unexpectedly, decidualization of primary endometrial stromal cells (EnSCs) was associated with a 60% reduction in O-GlcNAc modified proteins, reflecting downregulation of the enzyme that adds O-GlcNAc to substrates (O-GlcNAc transferase, OGT) but not the enzyme that removes the modification (O-GlcNAcase, OGA). Notably, EOGT, an endoplasmic reticulum-specific O-GlcNAc transferase that modifies a limited number of secreted and membrane proteins, was markedly induced in differentiating EnSCs. Knockdown of EOGT perturbed a network of decidual genes involved in multiple cellular functions. The most downregulated gene upon EOGT knockdown in decidualizing cells was *ENHO*, which encodes adropin, a metabolic hormone involved in energy homeostasis and glucose and fatty acid metabolism. Analysis of mid-luteal endometrial biopsies revealed an inverse correlation between endometrial *EOGT* and *ENHO* expression and body mass index. Taken together, our findings reveal that obesity impairs the EOGT-adropin axis in decidual cells, which in turn points towards a novel mechanistic link between metabolic disorders and adverse pregnancy outcome.

Précis

Induction of EOGT, a selective glycosyltransferase downstream of the nutrient-dependent hexosamine biosynthetic pathway, is essential for endometrial decidualization and adropin expression.

Introduction

During the mid-luteal phase of the menstrual cycle, the endometrium becomes transiently poised to transit from a cycling into a semi-permanent tissue that is maintained throughout pregnancy (1). During this window, the luminal endometrial epithelial cells acquire a receptive phenotype and the underlying stromal cells start to differentiate into secretory decidual cells. After breaching of the luminal epithelium, migratory decidual cells rapidly encapsulate the implanting embryo (2), and form a nutritive and immune-privileged matrix that enables trophoblast invasion and placenta formation (3). Once the process of interstitial and endovascular trophoblast invasion begins, the placental-maternal interface is intensely remodeled and exposed to profound changes fluctuations in oxygen tension associated with changes to the vascular tree (1,4). Decidual cells are programmed to resist a range of stressors, thus ensuring integrity of the interface and survival of the conceptus. Several molecular mechanisms underpin this quasi-autonomous state of decidua cells, including silencing of circadian gene expression (5), inhibition of stress pathways such as c-Jun N-terminal kinase (JNK) (4,6), attenuated inositol trisphosphate signaling (7), global cellular hypoSUMOylation (8), resistance to miRNA-mediated gene silencing through loss of argonaute proteins (9), and marked upregulation of free radical scavengers (10).

Posttranslational modification of proteins with O-linked β-N-acetylglucosamine (O-GlcNAc) is an integral component of the cellular stress response (11,12). O-GlcNAcylation refers to the covalent addition of a GlcNAc sugar moiety to hydroxyl groups of serine and/or threonine residues of cytosolic, nuclear, and mitochondrial proteins. The O-GlcNAc transferase (OGT) transfers the O-GlcNAc moiety from uridine diphosphate (UDP)-GlcNAc to target proteins, whereas O-GlcNAcase (OGA) removes O-GlcNAc from proteins. UDP-GlcNAc is an end product of the nutrient-dependent hexosamine biosynthetic pathway (HBP), a branch pathway in glycolysis. Increased glucose flux through the HBP elevates UDP-GlcNAc

and drives increased cellular O-GlcNAcylation (13,14). OGT targets in excess of 3,000 proteins (15), enabling it to regulate multiple processes, including signal transduction and transcription in a manner akin to - and cooperative with - protein phosphorylation (11,16). Importantly, increased O-GlcNAcylation is important for cell survival in response to a variety of stressors, including osmotic (12,17), oxidative (18), genotoxic (12,19,20), endoplasmic reticulum (ER) (21), and hypoxia/re-oxygenation stress (21,22).

In addition to OGT, a second enzyme has been identified that catalyzes the transfer of GlcNAc from UDP-GlcNAc to epidermal growth factor (EGF) repeats of extracellular proteins was identified (23,24). By contrast to OGT, this glycosyltransferase, termed EGF domain-specific O-linked GlcNAc transferase (EOGT), resides in the ER and targets seemingly only a very limited number of secreted and membrane receptors, including Notch receptors (25-27).

In this study, we examined the expression OGT, OGA and EOGT upon decidual transformation of primary EnSCs. Although increased O-GlcNAcylation has been implicated in stress resistance, decidualization was associated with a marked reduction in O-GlcNAc-modified proteins, reflecting down-regulation of OGT but not OGA. However, EOGT expression in differentiating EnSCs was increased. While the EOGT target proteins in decidual cells remain to be determined, we demonstrate that EOGT knockdown perturbs the expression of numerous genes; most prominently *ENHO*, which encodes a newly discovered metabolic hormone, adropin, that regulates lipid metabolism, confers insulin sensitivity, and protects against vascular disease (28,29). Finally, we demonstrate that obesity, a major risk factor for reproductive failure, is associated with lower mid-luteal endometrial EOGT and adropin expression.

Methods

Patient selection and endometrial sampling

The study was approved by the NHS National Research Ethics – Hammersmith and Queen Charlotte's & Chelsea Research Ethics Committee (1997/5065). Endometrial samples were obtained during the luteal phase of an ovulatory, non-hormonally stimulated menstrual cycle using a Wallach Endocell^{TM} sampler, starting from the uterine fundus and moving downward to the internal cervical ostium. Written informed consent was obtained from all participants in accordance with the guidelines in The Declaration of Helsinki 2000. A total of 193 biopsies were used in this study, including 24 fresh endometrial biopsies processed for primary culture. In addition, 112 biopsies stored in RNAlater (Sigma-Aldrich) were used to measure mRNA expression and a further 57 snap-frozen and formalin-fixed biopsies were used for Western blot analysis and immunohistochemistry, respectively. All endometrial biopsies were timed between 6 and 10 days after the pre-ovulatory LH surge. Demographic details are summarized in Supplementary Table 1. None of the subjects was on hormonal treatment for at least 3 months prior to the procedure.

Primary cell culture

EnSCs were isolated and established from endometrial tissues as described previously (30). Confluent EnSC monolayers were decidualized in DMEM/F-12 containing 2% DCC-FBS with 0.5 mM 8-bromo-cAMP (Sigma-Aldrich) and 10^{-6} M medroxyprogesterone acetate (MPA; Sigma-Aldrich) to induce a differentiated phenotype. Culture medium was refreshed every 48 hours. All experiments were carried out before the third cell passage.

Transient transfections

Primary EnSCs were transfected with small interfering RNA (siRNA) using the jetPRIME Polyplus transfection kit (VWR International). Undifferentiated EnSCs were transiently transfected with 50 nM EOGT-siGENOME SMARTpool or siGENOME Non-Targeting (NT) siRNA Pool 1 (GE Healthcare). Transfection studies were performed in triplicate and repeated on primary cultures from 4 subjects.

Real-time quantitative (RTQ)-PCR

Total RNA was extracted from EnSC cultures using RNA STAT-60 (AMS Biotechnology). Equal amounts of total RNA were treated with DNase and reverse transcribed using the QuantiTect Reverse Transcription Kit (QIAGEN) and the resulting cDNA used as template in qRT-PCR analysis. Detection of gene expression was performed with Power SYBR® Green Master Mix and the 7500 Real Time PCR System. The expression levels of the samples were calculated using the dCt method, incorporating the efficiencies of each primer pair. The variances of input cDNA were normalized against the levels of the *L19* housekeeping gene. All measurements were performed in triplicate. Melting curve analysis confirmed product specificity.

Western blot analysis

Protein extracts were prepared by lysing cells in RIPA buffer containing protease inhibitors (cOmplete, Mini, EDTA-free; Roche). Protein yield was quantified using the Bio-Rad Protein Assay Dye Reagent Concentrate. Equal amounts of protein were separated by SDS-Polyacrylamide Gel Electrophoresis (SDS-PAGE) before wet-transfer onto nitrocellulose membrane. Global O-GlcNAcylation was determined by spotting 10 µg and 2 µg of total protein lysate directly onto nitrocellulose membranes. Nonspecific binding sites were blocked by overnight incubation with 5% non-fat dry milk in Tris-buffered saline with 1% Tween

(TBS-T; 130 mmol/L NaCl, 20 mmol/L Tris, pH7.6 and 1% Tween). The antibodies used in this study are listed in Table 1. Protein complexes were visualized with ECL Plus chemiluminescence. Densitometry was performed using Gene Tools software.

Immunohistochemistry

Paraffin-embedded, formalin fixed endometrial specimens were immunostained for EOGT using the Novolink polymer detection systems (Leica) as per manufacturer's instructions. Universal LSAB Plus kits (DAKO) were used as previously described (31) using primary antibodies against EOGT (1:500 dilution) and ENHO (1:200 dilution). Bright-field imagines were obtained on a Mirax Midi slide scanner and visualized using Panoramic Viewer software for analysis.

RNA-Sequencing and data analysis

Total RNA was extracted using RNA-STAT-60 from primary EnSC cultures first transfected with either EOGT or non-targeting (NT) siRNA and then decidualized with 8-br-cAMP and MPA for 4 days. 3 biological repeats were performed to allow for inter-patient variability. RNA quality was analysed on an Agilent 2100 Bioanalyzer. RNA integrity number score for all samples was ≥ 8.0. Transcriptomic maps of paired-end reads were generated using Bowtie-2.2.3, SAMtools 0.1.19, and TopHat 2.0.12 against the University of California, Santa Cruz hg19 reference transcriptome (2014) from the Illumina iGenomes resource using the fr-firststrand setting. Transcript counts were assessed by HTSeq-0.6.1. Transcripts per million (TPM) were calculated as recently described (32). Differential gene expression analysis was performed using DEseq2-1.14.1. Significance was defined as an adjusted *P* value (*q* value) of < 0.05 following Benjamini-Hochberg False Discovery Rate correction. Expression data have been submitted to the Gene Expression Omnibus (GEO) repository (accession number:

GSE104720). Gene Ontology (GO) analyses were carried out using DAVID Bioinformatics Resources 6.8 (33,34) and visualized using REVIGO online software (35). GO Term Gene Set Enrichment Analysis (GSEA), was performed using piano R package (36). Briefly, GO ID was extracted for each Ensembl gene ID using biomaRt package in R (37). Gene ID and GO ID were loaded into correct format using loadGSC function and GSEA was performed using the runGSA function. Genes were ranked according to the adjusted *P* value and log2 Fold Change was used to determine up or downregulated transcripts.

Statistical Analysis

In vitro experiments were analyzed with the statistical package Graphpad Prism 6. Unpaired Student's *t*-test and one-way ANOVA with post hoc Tukey's test were used when appropriate. The association between *EOGT* and *ENHO* mRNA in endometrial biopsies and BMI was analyzed using Pearson's rank correlation. Statistical significance was assumed when $P < 0.05$

Results

Loss of OGT-dependent O-GlcNAcylation in decidualizing EnSCs

O-GlcNAcylation of target proteins is enhanced in response to diverse stress signals and tissue injury (15). To test if O-GlcNAcylation plays a role in decidualization, primary EnSCs were decidualized with 8-br-cAMP and MPA for 2, 4 or 8 days and the expression of O-GlcNAc processing enzymes, OGT, EOGT and OGA, examined at both mRNA and protein level. Analysis of 4 independent primary cultures demonstrated that decidualization results in downregulation of the canonical O-GlcNAc transferase OGT at both mRNA and protein level (Fig. 1A and 1B), whereas expression of OGA (encoded by *MGEA5*) was unchanged. In contrast to OGT, expression of EOGT increased significantly upon decidualization. In fact, induction of EOGT was more marked at protein than mRNA level, with levels increasing ~5-fold after 8 days of decidualization (Fig. 1A and 1B). Densitometric analyses of Western blots are shown in Supplementary Fig. 1.

While thousands of OGT substrates have been identified, only a handful of EOGT targets have been described to date (38,39). To determine the impact of decidualization on total cellular O-GlcNAcylation, protein lysates from undifferentiated EnSCs and cells decidualized for 8 days were subjected to dot-blot analysis using a primary antibody directed against serine and threonine residues with attached beta-O-linked GlcNAc. This analysis revealed ~60% reduction in global O-GlcNAcylation in decidual cells (Fig. 1C), reflecting the relative shift to OGA over OGT. Thus, decidualization is associated with decreased OGT-mediated cellular O-GlcNAcylation, yet increased expression of EOGT, a highly selective transferase that targets secreted and membrane-bound proteins (39).

EOGT expression in mid-luteal endometrium.

Mining of the Genotype-Tissue Expression (GTEx) and FANTOM (Functional Annotation of Mammalian Genomes) projects revealed that *EOGT* is highly expressed in the endometrium compared to other tissues (40,41). Furthermore, analysis of Gene Expression Omnibus (GEO profile ID: 24476716) demonstrated that *EOGT* mRNA levels in cycling endometrium increases sharply upon transition from the early- to mid-secretory endometrium (Fig. 2A). Laser microdissection of glandular endometrial epithelium coupled to RNA-sequencing revealed a transient 3-fold increase in *EOGT* mRNA levels during the mid-luteal phase, coinciding with the putative window of implantation (Fig. 2B) (42). Immunohistochemistry was performed to assess the spatiotemporal expression of EOGT in the endometrial stromal compartment. In timed early-secretory phase (LH+5) biopsies, EOGT immunoreactivity was largely confined to endometrial glands (Fig. 2C, upper panel). During the mid-luteal implantation window (LH+9), stromal cells were strongly EOGT positive (Fig 2C, lower panel). Interestingly, EOGT was also expressed in endothelial cells lining the emerging terminal spiral arteries, although the surrounding perivascular cells often appeared devoid of this glycosyltransferase. Thus, EOGT is expressed in the endometrial epithelial compartment, decidualizing stromal cells and vascular endothelial cells at the time of embryo implantation

Impact of EOGT knockdown on decidual marker genes and Notch signaling.

Induction of decidual marker genes, such as *PRL* and *IGFBP1*, in response to cAMP and progestin signaling is mediated, at least in part, by the auto/paracrine actions of a host of cytokines and morphogens (1). We speculated that the strong induction of EOGT could be essential for the expression of decidual marker genes in differentiating EnSCs. To test this conjecture, 4 primary cultures were first transfected with non-targeting (NT) or EOGT siRNA and then decidualized with 8-br-cAMP and MPA for 2, 4 or 8 days. Although EOGT knockdown was highly efficient (Fig. 3A, upper panel), there was no significant impact on the

induction of either *PRL* or *IGFBP1* in decidualizing cultures (Fig. 3A, middle and lower panels, respectively).

Notch receptors are perhaps the best characterized targets of EOGT (27). O-GlcNAc modification of epidermal growth factor-like repeats of NOTCH1 enhances signaling by potentiating interaction with Delta like-1 (DLL1) and DLL4 ligands in a cell-specific context (27). Ligand binding to the extracellular domain of Notch receptors induces proteolytic cleavage and releases Notch intracellular domain (ICD), which enters the cell nucleus to regulate gene expression. To test if induction of EOGT in decidualizing EnSCs modulates Notch signaling, total protein lysates of undifferentiated cells and cells treated with 8-br-cAMP and MPA for 2, 4 or 8 days were subjected to Western blot analysis for NOTCH1 and NOTCH3 ICDs. As shown in Figure 3B, decidualization was associated with gradual silencing of Notch signaling and EOGT knockdown had no discernable effect on this response. Further, expression of *HEY1* and *HES1*, target genes of the canonical Notch signaling pathway (43), was not significantly altered upon EOGT knockdown in EnSCs decidualized for 4 days ($P > 0.05$; Fig. 3C). Taken together, these observations indicate that Notch activity is not likely regulated by EOGT-mediated O-GlcNAcylation in decidualizing cells.

EOGT knockdown perturbs decidual gene expression.

To gain insight in the role of EOGT in decidual cells, total RNA harvested from 3 independent cultures, first transfected with either EOGT or NT siRNA and then treated with 8-br-cAMP and MPA for 4 days, was subjected to RNA sequencing. Approximately, 26-36 million paired-end reads were sequenced per sample. After accounting for variation between primary cultures, the impact of EOGT knockdown on decidual gene expression was highly consistent with principal components (PC) 1 and 2 accounting for 52% and 36% of variance in gene expression, respectively (Fig. 4A). Based on $q \leq 0.05$, we identified 340 genes that were

significantly altered upon EOGT knockdown (Fig. 4B); of which 178 (52%) were up- and 162 (48%) down-regulated. Several highly induced decidual genes were downregulated significantly upon EOGT knockdown, including *LEFTY2* ($q = 3.13 \times 10^{-4}$), *CDKN1C* ($q = 5.10 \times 10^{-8}$), *GADD45G* ($q = 9.58 \times 10^{-9}$) and *GPX3* ($q = 7.17 \times 10^{-12}$) (Supplementary Fig. 2). EOGT knockdown also downregulated *ESR1*, coding the estrogen receptor alpha, in decidualizing cells ($q = 1.07 \times 10^{-3}$). However, the most repressed gene upon EOGT knockdown was *ENHO* (Energy Homeostasis Associated gene; -2.03 log2 fold-change; $q = 5.67 \times 10^{-11}$), coding adropin, a recently discovered peptide hormone implicated in the regulation of energy homeostasis, insulin resistance and lipid metabolism (28). Interestingly, *IL1RL1*, which encodes the IL-33 receptor, is strongly upregulated upon decidualization (44), yet EOGT knockdown amplified induction of this gene in differentiating EnSCs (1.8 log2 fold-change; $q = 2.31 \times 10^{-17}$).

Gene ontology (GO) term enrichment analysis, using both DAVID (Fig. 4C) and GSEA (Supplementary Fig. 3), revealed that EOGT knockdown results in upregulation of genes involved - amongst other categories - in cell adhesion, extracellular matrix organization, and signal transduction (Fig 4C, left panel; Supplementary Table 2; Supplementary Fig. 3). Notable GO terms enriched in downregulated genes include oxidative-reductive process, response to estrogen/estradiol, and inflammatory responses (Fig 4C, right panel; Supplementary Table 2; Supplementary Fig. 3). We also annotated genes perturbed upon EOGT knockdown by their disease association. GO analysis yielded a conspicuous association between EOGT-responsive decidual genes and vascular and metabolic disorders, most prominently type 2 diabetes (Fig. 4D).

Obesity perturbs the endometrial EOGT-adropin axis

To explore the putative link with metabolic disorders, we measured EOGT transcript level by RTQ-PCR in 112 mid-luteal (LH+7-10) endometrial biopsies. Demographic details are summarized in Supplementary Table 1. Interestingly, endometrial *EOGT* mRNA levels correlated inversely with body mass index (BMI) (Pearson's r = -0.194, $P = 0.043$; Fig. 5A). By contrast, no association was found between either *OGT* or *OGA* mRNA levels and BMI (Supplementary Fig. 4). Western blot analysis of total protein lysates of 48 biopsies (LH+7-9) substantiated the inverse correlation between endometrial EOGT levels and BMI (r = -0.335, $P = 0.02$; Fig. 5B), with levels being significantly lower in clinically obese patients compared to control subjects ($P < 0.03$) (Fig. 5C).

Expression of adropin in the endometrium has not yet been reported. As shown in Figure 6A, *ENHO* mRNA levels increase significantly in primary EnSCs decidualized with 8-br-cAMP and MPA for 4 days, although the level of induction varied markedly between primary cultures (Fig. 6A, Supplementary Fig. 5). Furthermore, immunohistochemistry of serial endometrial sections (LH+8) revealed that the tissue distribution of adropin is indistinguishable from EOGT, characterized by strong expression in glands, differentiating stromal cells, and endothelial but not perivascular cells (Fig. 6B). Furthermore, a strong positive correlation was observed between *EOGT* and *ENHO* transcript levels in 112 timed endometrial biopsies (r = 0.327, $P = 0.0003$; Fig. 6C); as well as a negative correlation between *ENHO* mRNA expression and BMI (r = -0.178, $P = 0.044$; Fig. 6D).

Discussion

Dynamic changes in protein O-GlcNAcylation enable cells to homeostatically balance energy supply and demand by modulating the stability, localization and function of a myriad of proteins (45). Here, we report that decidualizing EnSCs downregulate OGT expression and intracellular O-GlcNAcylation but upregulate the highly selective glycosyltransferase EOGT.

Increased canonical O-GlcNAcylation is a well characterized pro-survival response (15); rendering the downregulation of OGT in differentiating EnSCs counterintuitive, especially as initiation of decidual differentiation coincides with a burst of endogenous reactive oxygen species (ROS) production and release of various inflammatory mediators (46,47). However, SUMO modification of proteins is also dramatically reduced in decidualizing cells and uncoupled from JNK-mediated stress signaling though the induction of MAP kinase phosphatase 1 (MKP1) (48-50). Hence, by silencing selective pathways that converge on the posttranslational modification code of numerous proteins, decidual cells appear to prioritize cellular homeostasis over an adaptive response to stress signals. Further, recent studies have shown that decidualization is critically dependent on glucose utilization via the pentose phosphate pathway (51), suggesting that loss of OGT may be integral to the metabolic reprogramming of the endometrium in preparation of pregnancy.

Induction of EOGT in the endometrium during the mid-luteal phase of the cycle coincides with the window of implantation. At this time, EOGT is expressed in the glandular epithelium, vascular endothelial cells, and stromal cells that are poised to decidualize. Decidualization is characterized by an unfolded protein response that underpins ER expansion and acquisition of a secretory phenotype (52). In fact, multiple secreted factors, including interleukin (IL)-11, leukemia inhibitory factor (LIF) and bone morphogenetic protein 2 (BMP2), have been implicated in the auto/paracrine propagation of the decidual response (1). However, the identity and role of EOGT target proteins, whether secreted or expressed on the cell surface, in differentiating EnSCs requires further investigation. We showed that Notch signaling is attenuated upon decidualization (53), irrespective of EOGT knockdown. Furthermore, other known EOGT target proteins (26), including thrombospondin (THBS1), peptidase domain containing associated with muscle regeneration 1 (PAMR1), and laminin alpha 5 (LAMA5), are also downregulated upon decidualization, at least at mRNA level (GEO

accession number: GSE104720). Although EOGT knockdown did not significantly impact on *PRL* or *IGFBP1* expression in differentiating cells, RNA-sequencing uncovered a robust set of 341 EOGT-dependent genes. EOGT knockdown upregulated several genes encoding inflammatory mediators, including IL-1β (*IL1B*) and complement component 3 (*C3*), but downregulated key genes involved in decidual stress defenses, such as *GPX3* (coding extracellular glutathione peroxidase), *GLXR* (glutaredoxin) and *GADD45G* (growth arrest and DNA damage inducible gamma) (1). EOGT knockdown also blunted the induction of other cardinal decidual genes, including *F3* (tissue factor) (1), *LEFTY2* (left-right determination factor 2, also known as endometrial bleeding-associated factor or EBAF) (54), and *CDKN1C* (cyclin dependent kinase inhibitor 1C, $p57^{kip2}$) (55). Most strikingly, however, was the repression of *ENHO* upon loss of EOGT. *ENHO* encodes adropin, a recently discovered peptide hormone implicated in energy homeostasis, glucose and fatty acid metabolism, and vascular protection (56). Although *ENHO* is primarily expressed in the liver, pancreas and brain (28), we showed that this gene is also induced upon decidualization of human EnSCs, although the magnitude of induction varied markedly between primary cultures. We further showed a strong positive correlation between *EOGT* and *ENHO* transcript levels in whole endometrial biopsies; and immunohistochemistry on serial tissue sections revealed that the cellular distribution of adropin in mid-luteal endometrium is indistinguishable from EOGT.

GO analysis revealed a putative association between decidual genes perturbed upon EOGT knockdown and metabolic and cardiovascular disorders. To explore this possible link further, we measured the transcript levels of the 3 O-GlcNAc processing enzymes in 112 randomly selected mid-luteal endometrial biopsies from women ranging in BMI from 18 to 42. A weak but significant negative correlation was observed between BMI and *EOGT* mRNA levels but not *OGT* or *OGA* expression. Western blot analysis confirmed that obesity is

associated with impaired endometrial EOGT expression. Furthermore, endometrial *ENHO* transcript levels also correlated negatively with BMI.

Obesity increases the risk of a spectrum of pregnancy disorders, including obstetrical syndromes, such as pre-eclampsia, fetal growth restriction and preterm labor (57,58), that are caused by impaired endovascular trophoblast invasion and spiral artery remodeling (59). In the absence of physiological remodeling, these uterine vessels are prone to develop acute atherosis, characterized by changes in lipid metabolism, intravascular inflammation, macrophage infiltration and endothelial cell dysfunction (60). Adropin promotes various indices of vascular health, including increased endothelial cell proliferation, migration, and angiogenesis; and diminishes permeability and apoptosis (61). Although as yet untested, these observations suggest that adequate decidual adropin production may be essential for successful spiral artery remodeling in pregnancy. Notably, low circulating adropin levels have not only been associated with high BMI, insulin resistance, endothelial dysfunction and coronary atherosclerosis but also severe preeclampsia (62,63).

In summary, the shift from OGT to EOGT dominance in decidualizing EnSCs results in intracellular hypo-O-GlcNAcylation whereas glucose utilization through the HBP pathway for modification of selective secreted and/or membrane proteins is likely enhanced. We demonstrate that EOGT upregulation is critical for normal decidual function and identified *ENHO* as major EOGT-responsive gene. Further, our observation that obesity impairs the EOGT-adropin axis in the endometrium intimates a novel mechanistic pathway that links metabolic disorders to vascular placental pathology and adverse pregnancy outcome.

Acknowledgement

We are grateful to all participating women. We also like to thank Drs Siobhan Quenby and David Snead for valuable advice. This study was funded by Diabetes UK (15/0005207) and Tommy's National Miscarriage Research Centre.

References

1. Gellersen B, Brosens JJ. Cyclic decidualization of the human endometrium in reproductive health and failure. Endocrine reviews 2014; 35:851-905
2. Weimar CH, Kavelaars A, Brosens JJ, Gellersen B, de Vreeden-Elbertse JM, Heijnen CJ, Macklon NS. Endometrial stromal cells of women with recurrent miscarriage fail to discriminate between high-and low-quality human embryos. PLoS One 2012; 7:e41424
3. Erlebacher A. Immunology of the maternal-fetal interface. Annual review of immunology 2013; 31:387-411
4. Leitao BB, Jones MC, Brosens JJ. The SUMO E3-ligase PIAS1 couples reactive oxygen species-dependent JNK activation to oxidative cell death. The FASEB Journal 2011; 25:3416-3425
5. Muter J, Lucas ES, Chan Y-W, Brighton PJ, Moore JD, Lacey L, Quenby S, Lam EWF, Brosens JJ. The clock protein period 2 synchronizes mitotic expansion and decidual transformation of human endometrial stromal cells. The FASEB Journal 2015; 29:1603-1614
6. Leitao B, Jones MC, Fusi L, Higham J, Lee Y, Takano M, Goto T, Christian M, Lam EWF, Brosens JJ. Silencing of the JNK pathway maintains progesterone receptor activity in decidualizing human endometrial stromal cells exposed to oxidative stress signals. Faseb Journal 2010; 24
7. Muter J, Brighton PJ, Lucas ES, Lacey L, Shmygol A, Quenby S, Blanks AM, Brosens JJ. Progesterone-dependent induction of phospholipase c-related catalytically inactive protein 1 (prip-1) in decidualizing human endometrial stromal cells. Endocrinology 2016; 157:2883-2893
8. Jones MC, Fusi L, Higham JH, Abdel-Hafiz H, Horwitz KB, Lam EWF, Brosens JJ. Regulation of the SUMO pathway sensitizes differentiating human endometrial stromal cells to progesterone. Proceedings of the National Academy of Sciences of the United States of America 2006; 103:16272-16277
9. Shah KM, Webber J, Carzaniga R, Taylor DM, Fusi L, Clayton A, Brosens JJ, Hartshorne G, Christian M. Induction of microRNA resistance and secretion in differentiating human endometrial stromal cells. J Mol Cell Biol 2013; 5:67-70
10. Kajihara T, Jones M, Fusi L, Takano M, Feroze-Zaidi F, Pirianov G, Mehmet H, Ishihara O, Higham JM, Lam EWF. Differential expression of FOXO1 and FOXO3a

confers resistance to oxidative cell death upon endometrial decidualization. Molecular endocrinology 2006; 20:2444-2455

11. Butkinaree C, Park K, Hart GW. O-linked β-N-acetylglucosamine (O-GlcNAc): extensive crosstalk with phosphorylation to regulate signaling and transcription in response to nutrients and stress. Biochimica et Biophysica Acta (BBA)-General Subjects 2010; 1800:96-106

12. Zachara NE, O'Donnell N, Cheung WD, Mercer JJ, Marth JD, Hart GW. Dynamic O-GlcNAc modification of nucleocytoplasmic proteins in response to stress A survival response of mammalian cells. Journal of Biological Chemistry 2004; 279:30133-30142

13. Walgren JLE, Vincent TS, Schey KL, Buse MG. High glucose and insulin promote O-GlcNAc modification of proteins, including α-tubulin. American Journal of Physiology-Endocrinology and Metabolism 2003; 284:E424-E434

14. Housley MP, Rodgers JT, Udeshi ND, Kelly TJ, Shabanowitz J, Hunt DF, Puigserver P, Hart GW. O-GlcNAc regulates FoxO activation in response to glucose. Journal of Biological Chemistry 2008; 283:16283-16292

15. Groves JA, Lee A, Yildirir G, Zachara NE. Dynamic O-GlcNAcylation and its roles in the cellular stress response and homeostasis. Cell Stress and Chaperones 2013; 18:535-558

16. Wang Z, Gucek M, Hart GW. Cross-talk between GlcNAcylation and phosphorylation: site-specific phosphorylation dynamics in response to globally elevated O-GlcNAc. Proceedings of the National Academy of Sciences 2008; 105:13793-13798

17. Zou L, Yang S, Hu S, Chaudry IH, Marchase RB, Chatham JC. The protective effects of PUGNAc on cardiac function after trauma-hemorrhage are mediated via increased protein O-GlcNAc levels. Shock 2007; 27:402-408

18. Jones SP, Zachara NE, Ngoh GA, Hill BG, Teshima Y, Bhatnagar A, Hart GW, Marbán E. Cardioprotection by N-acetylglucosamine linkage to cellular proteins. Circulation 2008; 117:1172-1182

19. Zachara NE, Molina H, Wong KY, Pandey A, Hart GW. The dynamic stress-induced "O-GlcNAc-ome" highlights functions for O-GlcNAc in regulating DNA damage/repair and other cellular pathways. Amino acids 2011; 40:793-808

20. Love DC, Ghosh S, Mondoux MA, Fukushige T, Wang P, Wilson MA, Iser WB, Wolkow CA, Krause MW, Hanover JA. Dynamic O-GlcNAc cycling at promoters of Caenorhabditis elegans genes regulating longevity, stress, and immunity. Proceedings of the National Academy of Sciences 2010; 107:7413-7418

21. Ngoh GA, Hamid T, Prabhu SD, Jones SP. O-GlcNAc signaling attenuates ER stress-induced cardiomyocyte death. American Journal of Physiology-Heart and Circulatory Physiology 2009; 297:H1711-H1719

22. Ngoh GA, Watson LJ, Facundo HT, Dillmann W, Jones SP. Non-canonical glycosyltransferase modulates post-hypoxic cardiac myocyte death and mitochondrial permeability transition. Journal of molecular and cellular cardiology 2008; 45:313-325

23. Matsuura A, Ito M, Sakaidani Y, Kondo T, Murakami K, Furukawa K, Nadano D, Matsuda T, Okajima T. O-linked N-acetylglucosamine is present on the extracellular domain of notch receptors. Journal of Biological Chemistry 2008; 283:35486-35495

24. Sakaidani Y, Nomura T, Matsuura A, Ito M, Suzuki E, Murakami K, Nadano D, Matsuda T, Furukawa K, Okajima T. O-Linked-N-acetylglucosamine on extracellular protein domains mediates epithelial cell–matrix interactions. Nature communications 2011; 2:583

25. Müller R, Jenny A, Stanley P. The EGF repeat-specific O-GlcNAc-transferase Eogt interacts with notch signaling and pyrimidine metabolism pathways in Drosophila. PloS one 2013; 8:e62835

26. Ogawa M, Furukawa K, Okajima T. Extracellular O-linked β-N-acetylglucosamine: Its biology and relationship to human disease. World journal of biological chemistry 2014; 5:224

27. Sawaguchi S, Varshney S, Ogawa M, Sakaidani Y, Yagi H, Takeshita K, Murohara T, Kato K, Sundaram S, Stanley P. O-GlcNAc on NOTCH1 EGF repeats regulates ligand-induced Notch signaling and vascular development in mammals. eLife 2017; 6:e24419

28. Aydin S. Three new players in energy regulation: preptin, adropin and irisin. Peptides 2014; 56:94-110

29. Mierzwicka A, Bolanowski M. New peptides players in metabolic disorders. Postepy higieny i medycyny doswiadczalnej (Online) 2016; 70:881-886

30. Barros FSV, Brosens JJ, Brighton PJ. Isolation and Primary Culture of Various Cell Types from Whole Human Endometrial Biopsies. Stem Cells 2016;

31. Feroze-Zaidi F, Fusi L, Takano M, Higham J, Salker MS, Goto T, Edassery S, Klingel K, Boini KM, Palmada M. Role and regulation of the serum-and glucocorticoid-regulated kinase 1 in fertile and infertile human endometrium. Endocrinology 2007; 148:5020-5029

32. Wagner GP, Kin K, Lynch VJ. Measurement of mRNA abundance using RNA-seq data: RPKM measure is inconsistent among samples. Theory in Biosciences 2012; 131:281-285

33. Huang DW, Sherman BT, Lempicki RA. Systematic and integrative analysis of large gene lists using DAVID bioinformatics resources. Nature protocols 2009; 4:44

34. Huang DW, Sherman BT, Lempicki RA. Bioinformatics enrichment tools: paths toward the comprehensive functional analysis of large gene lists. Nucleic acids research 2008; 37:1-13

35. Supek F, Bošnjak M, Škunca N, Šmuc T. REVIGO summarizes and visualizes long lists of gene ontology terms. PloS one 2011; 6:e21800

36. Väremo L, Nielsen J, Nookaew I. Enriching the gene set analysis of genome-wide data by incorporating directionality of gene expression and combining statistical hypotheses and methods. Nucleic acids research 2013; 41:4378-4391

37. Durinck S, Spellman PT, Birney E, Huber W. Mapping identifiers for the integration of genomic datasets with the R/Bioconductor package biomaRt. Nature protocols 2009; 4:1184-1191

38. Alfaro JF, Gong C-X, Monroe ME, Aldrich JT, Clauss TRW, Purvine SO, Wang Z, Camp DG, Shabanowitz J, Stanley P. Tandem mass spectrometry identifies many mouse brain O-GlcNAcylated proteins including EGF domain-specific O-GlcNAc transferase targets. Proceedings of the National Academy of Sciences 2012; 109:7280-7285

39. Varshney S, Stanley P. EOGT and O-GlcNAc on secreted and membrane proteins. Biochemical Society Transactions 2017; 45:401-408

40. Lonsdale J, Thomas J, Salvatore M, Phillips R, Lo E, Shad S, Hasz R, Walters G, Garcia F, Young N. The genotype-tissue expression (GTEx) project. Nature genetics 2013; 45:580-585

41. Lizio M, Harshbarger J, Shimoji H, Severin J, Kasukawa T, Sahin S, Abugessaisa I, Fukuda S, Hori F, Ishikawa-Kato S. Gateways to the FANTOM5 promoter level mammalian expression atlas. Genome biology 2015; 16:22

42. Salker MS, Singh Y, Zeng N, Chen H, Zhang S, Umbach AT, Fakhri H, Kohlhofer U, Quintanilla-Martinez L, Durairaj RRP. Loss of Endometrial Sodium Glucose Cotransporter SGLT1 is Detrimental to Embryo Survival and Fetal Growth in Pregnancy. Scientific reports 2017; 7:12612

514 **43.** Murakami K, Lee YH, Lucas ES, Chan Y-W, Durairaj RP, Takeda S, Moore JD, Tan
515 BK, Quenby S, Chan JKY. Decidualization induces a secretome switch in perivascular
516 niche cells of the human endometrium. Endocrinology 2014; 155:4542-4553
517 **44.** Salker MS, Nautiyal J, Steel JH, Webster Z, Sucurovic S, Nicou M, Singh Y, Lucas
518 ES, Murakami K, Chan YW, James S, Abdallah Y, Christian M, Croy BA, Mulac-
519 Jericevic B, Quenby S, Brosens JJ. Disordered IL-33/ST2 Activation in Decidualizing
520 Stromal Cells Prolongs Uterine Receptivity in Women with Recurrent Pregnancy Loss.
521 Plos One 2012; 7:18
522 **45.** Myslicki JP, Belke DD, Shearer J. Role of O-GlcNAcylation in nutritional sensing,
523 insulin resistance and in mediating the benefits of exercise. Applied Physiology,
524 Nutrition, and Metabolism 2014; 39:1205-1213
525 **46.** Al-Sabbagh M, Fusi L, Higham J, Lee Y, Lei K, Hanyaloglu AC, Lam EW, Christian
526 M, Brosens JJ. NADPH oxidase-derived reactive oxygen species mediate
527 decidualization of human endometrial stromal cells in response to cyclic AMP
528 signaling. Endocrinology 2011; 152:730-740
529 **47.** Lucas ES, Dyer NP, Murakami K, Lee YH, Chan YW, Grimaldi G, Muter J, Brighton
530 PJ, Moore JD, Patel G, Chan JK, Takeda S, Lam EW, Quenby S, Ott S, Brosens JJ.
531 Loss of Endometrial Plasticity in Recurrent Pregnancy Loss. Stem Cells 2016; 34:346-
532 356
533 **48.** Jones MC, Fusi L, Higham JH, Abdel-Hafiz H, Horwitz KB, Lam EW, Brosens JJ.
534 Regulation of the SUMO pathway sensitizes differentiating human endometrial stromal
535 cells to progesterone. Proc Natl Acad Sci U S A 2006; 103:16272-16277
536 **49.** Leitao B, Jones MC, Fusi L, Higham J, Lee Y, Takano M, Goto T, Christian M, Lam
537 EW, Brosens JJ. Silencing of the JNK pathway maintains progesterone receptor activity
538 in decidualizing human endometrial stromal cells exposed to oxidative stress signals.
539 FASEB J 2010; 24:1541-1551
540 **50.** Leitao BB, Jones MC, Brosens JJ. The SUMO E3-ligase PIAS1 couples reactive
541 oxygen species-dependent JNK activation to oxidative cell death. FASEB J 2011;
542 25:3416-3425
543 **51.** Frolova AI, O'neill K, Moley KH. Dehydroepiandrosterone inhibits glucose flux
544 through the pentose phosphate pathway in human and mouse endometrial stromal cells,
545 preventing decidualization and implantation. Molecular endocrinology 2011; 25:1444-
546 1455

52. Brosens JJ, Salker MS, Teklenburg G, Nautiyal J, Salter S, Lucas ES, Steel JH, Christian M, Chan YW, Boomsma CM, Moore JD, Hartshorne GM, Sucurovic S, Mulac-Jericevic B, Heijnen CJ, Quenby S, Koerkamp MJ, Holstege FC, Shmygol A, Macklon NS. Uterine selection of human embryos at implantation. Sci Rep 2014; 4:3894

53. Afshar Y, Miele L, Fazleabas AT. Notch1 is regulated by chorionic gonadotropin and progesterone in endometrial stromal cells and modulates decidualization in primates. Endocrinology 2012; 153:2884-2896

54. Tang M, Mikhailik A, Pauli I, Giudice LC, Fazelabas AT, Tulac S, Carson DD, Kaufman DG, Barbier C, Creemers JW, Tabibzadeh S. Decidual differentiation of stromal cells promotes Proprotein Convertase 5/6 expression and lefty processing. Endocrinology 2005; 146:5313-5320

55. Takano M, Lu Z, Goto T, Fusi L, Higham J, Francis J, Withey A, Hardt J, Cloke B, Stavropoulou AV, Ishihara O, Lam EW, Unterman TG, Brosens JJ, Kim JJ. Transcriptional cross talk between the forkhead transcription factor forkhead box O1A and the progesterone receptor coordinates cell cycle regulation and differentiation in human endometrial stromal cells. Mol Endocrinol 2007; 21:2334-2349

56. Kumar KG, Trevaskis JL, Lam DD, Sutton GM, Koza RA, Chouljenko VN, Kousoulas KG, Rogers PM, Kesterson RA, Thearle M. Identification of adropin as a secreted factor linking dietary macronutrient intake with energy homeostasis and lipid metabolism. Cell metabolism 2008; 8:468-481

57. Alanis MC, Goodnight WH, Hill EG, Robinson CJ, Villers MS, Johnson DD. Maternal super-obesity (body mass index≥ 50) and adverse pregnancy outcomes. Acta obstetricia et gynecologica Scandinavica 2010; 89:924-930

58. Brewer CJ, Balen AH. The adverse effects of obesity on conception and implantation. Reproduction 2010; 140:347-364

59. Brosens I, Pijnenborg R, Vercruysse L, Romero R. The "Great Obstetrical Syndromes" are associated with disorders of deep placentation. Am J Obstet Gynecol 2011; 204:193-201

60. Labarrere CA, DiCarlo HL, Bammerlin E, Hardin JW, Kim YM, Chaemsaithong P, Haas DM, Kassab GS, Romero R. Failure of physiologic transformation of spiral arteries, endothelial and trophoblast cell activation, and acute atherosis in the basal plate of the placenta. Am J Obstet Gynecol 2017; 216:287 e281-287 e216

580 **61.** Lovren F, Pan Y, Quan A, Singh KK, Shukla PC, Gupta M, Al-Omran M, Teoh H,
581 Verma S. Adropin is a novel regulator of endothelial function. Circulation 2010;
582 122:S185-192
583 **62.** Cakmak BD, Dundar B, Acikgoz AS, Ozgen G, Cift T, Ahmedian R, Altekin Y. The
584 relationship between maternal and umbilical cord adropin levels with the presence and
585 severity of preeclampsia. Journal of Perinatal Medicine 2017; 45:879-885
586 **63.** Wang H, Gao B, Wu Z, Wang H, Dong M. Alteration of serum adropin level in
587 preeclampsia. Pregnancy Hypertension: An International Journal of Women's
588 Cardiovascular Health 2017; 8:6-8
589 **64.** Salker MS, Singh Y, Zeng N, Chen H, Zhang S, Umbach AT, Fakhri H, Kohlhofer U,
590 Quintanilla-Martinez L, Durairaj RRP. Loss of Endometrial Sodium Glucose
591 Cotransporter SGLT1 is Detrimental to Embryo Survival and Fetal Growth in
592 Pregnancy. Scientific Reports 2017; 7
593

Figure 1. *Regulation of O-GlcNAcylation in decidualizing EnSCs*. A) *OGT, OGA* and *EOGT* transcript levels were measured in undifferentiated EnSCs and cells decidualized with 8-br-cAMP and MPA for 2, 4 or 8 days. Expression was normalized to *L19* mRNA levels and the data show mean ± SEM relative to that in undifferentiated cells in 4 independent primary cultures. Different letters above the error bars indicate groups are significantly different from each other at $P < 0.05$. Group comparison by ANOVA and post hoc Tukey's test. B) Total protein lysates from parallel cultures were subjected to Western blotting. β-Actin served as a loading control. C) Representative dot blot of total cellular O-GlcNAcylation from total protein lysates from cells decidualized for 2, 4 or 8 days. Lower panel denotes total cellular O-GlcNAcylation relative to β-actin by densitometry and expressed as arbitrary units (A.U.). Group comparison by ANOVA and post hoc Tukey's test.

Figure 2. *EOGT expression in mid-luteal endometrium.* A) *EOGT* transcripts, expressed as arbitrary units (A.U.) in proliferative (P), early secretory (ES), mid-secretory (MS) and late secretory (LS) endometrium. The data were derived from *in silico* analysis of GDS2052 microarray data. B) Expression of *EOGT*, in transcripts per million (TPM), in ES, MS and LS endometrial glandular epithelium. The data were derived from *in silico* analysis of published RNA-Seq data (64). Different letters above the error bars indicate groups are significantly different from each other at $P < 0.05$. Group comparison by ANOVA and post hoc Tukey's test. C) EOGT immunohistochemistry of mid-luteal endometrial biopsies obtained 5 and 9 days following the LH surge, representing the early- and mid-luteal phase, respectively. Inset in the upper panel shows no staining upon omission of primary antibody (negative control). Arrows indicate positive staining of endothelial cells. Scale bar = 50μm

Figure 3. *EOGT knockdown in decidualizing EnSCs.* A) Four independent primary cultures were transfected with either non-targeting siRNA (siNT) or siRNA targeting EOGT (siEOGT). After 24 hours, the cultures remained either undifferentiated or were decidualized for 2, 4 and 8 days. Total mRNA was subjected to RTQ-PCR analysis to determine transcript levels for *EOGT* (left panel), *PRL* (middle panel) and *IGFBP1* (right panel). Expression was normalized to *L19* mRNA levels and data show mean ± SEM fold change relative to undifferentiated EnSCs. ** $P < 0.01$. Group comparison by Unpaired t test. B) Western blot analysis of EOGT, NOTCH1 and NOTCH3 ICDs levels in total protein lysates from EnSCs first transfected with siNT or siEOGT and then decidualized for the indicated time points. β-Actin served as a loading control. Densitometric analyses of NOTCH1 and NOTCH3 expression are shown in middle and right panels, respectively. C) Transcript expression of *HES1* and *HEY1*, normalized to *L19* mRNA, from 3 independent primary EnSC cultures transfected with siNT or siEOGT and decidualized for 4 days. Data are mean ± SEM of three biological replicates. $P > 0.05$ (unpaired *t*-test).

Figure 4. EOGT *knockdown perturbs distinct gene networks in EnSCs.* A) Principal Component Analysis of RNA-Seq data from 3 independent primary EnSC cultures first transfected with siNT and siEOGT and then decidualized for 4 days. B) Clustered heatmap of RNA-seq data for differentially expressed transcripts between siEOGT and siNT transfected cultures. C) Semantic clustering of significantly overrepresented GO terms ($P < 0.05$) of differentially up- and down-regulated genes (left and right panel, respectively) upon *EOGT* knockdown. Circle size is proportional to the percentage of genes in the GO term whereas the color indicates the log10 p-value. Color key is on the right. D) Word cloud presentation of overrepresented disease associations based on GO terms upon *EOGT* knockdown in decidualizing EnSCs. Size of word is proportional to log10 q-value.

643

644 **Figure 5.** *Obesity perturbs endometrial EOGT expression.* A) Pearson's correlation (r)
645 between normalized *EOGT* transcript levels in mid-luteal endometrial biopsies and BMI in 112
646 subjects. B) Pearson's correlation between normalized EOGT protein expression and BMI in
647 mid-luteal endometrial biopsies from 48 subjects. C) Normalized EOGT protein levels in timed
648 endometrial biopsies obtained from women with BMIs of <25, 25-30 (overweight), and > 30
649 (obese). * $P < 0.05$ (unpaired *t*-test).

650

651 **Figure 6.** *Endometrial ENHO expression relates to BMI* A) *ENHO* mRNA levels were
652 measured in undifferentiated EnSCs and cells decidualized with 8-br-cAMP and MPA for 4
653 days (upper panel). Expression was normalized to *L19* mRNA levels and the data show fold-
654 change relative to expression in undifferentiated cells in 6 independent primary cultures ** P
655 < 0.01 (unpaired *t*-test). Total protein lysates from parallel cultures were subjected to Western
656 blotting (lower panel). β-Actin served as a loading control. B) Immunohistochemistry of EOGT
657 (left panel) and adropin (right panel) on serial tissue sections, demonstrating co-localization of
658 both proteins in mid-luteal endometrium. Inset in the left panel shows no staining upon
659 omission of primary antibody (negative control); arrows indicate EOGT and adropin
660 immunoreactivity in endothelial cells of terminal spiral arteries. Scale bars = 50μm. C)
661 Pearson's correlation between *EOGT* and *ENHO* transcripts in endometrial biopsies from 112
662 subjects. D) Pearson's correlation between *ENHO* mRNA levels in mid-luteal endometrial
663 biopsies and BMI in 112 subjects.

664

665

666

667

668 **Table 1:** Primary Antibodies used throughout the study.

Protein Target	Manufacturer and Catalogue number	Dilution	Research Resource Identifier
OGT	CST # 24083	WB 1:1000	AB_2716710
OGA	Sigma-Aldrich #SAB4200267	WB 1:500	AB_10797267
EOGT	Sigma-Aldrich #HPA019460	WB 1:500; IHC 1:500	AB_1844628
O-GlcNAc (CTD110.6)	Sigma-Aldrich #O7764	WB 1:500	AB_1079524
NOTCH1	CST # 3608	WB 1:1000	AB_10691684
NOTCH3	CST # 5276	WB 1:1000	AB_10560515
ADROPIN	Abcam #ab122800	WB 1:500; IHC 1:300	AB_11132112
B-ACTIN	Abcam #ab8227	WB 1:50000	AB_2305186

669

670

Figure 1:

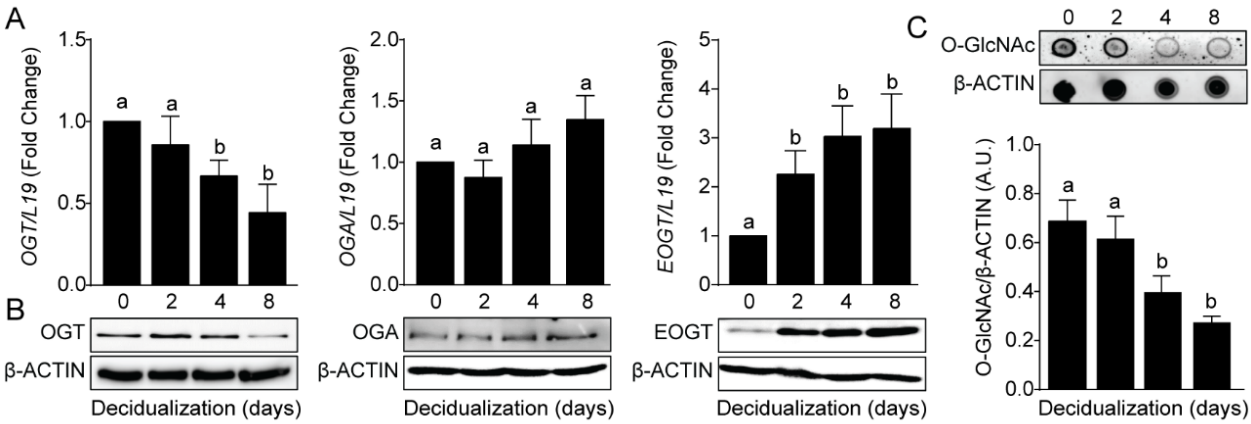
A
OGT/L19 (Fold Change)
OGA/L19 (Fold Change)
EOGT/L19 (Fold Change)
B
OGT
OGA
EOGT
β-ACTIN
Decidualization (days)
C
O-GlcNAc
β-ACTIN
O-GlcNAc/β-ACTIN (A.U.)
Decidualization (days)

Figure 2:

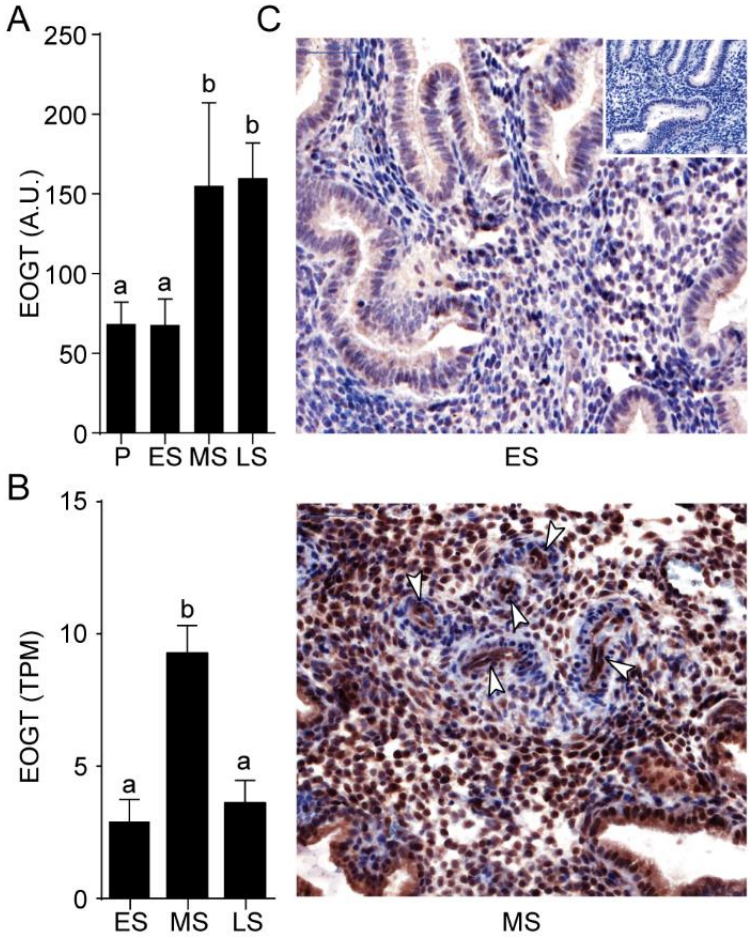
A
250
200
150
100
50
0
EOGT (A.U.)
a
a
b
b
P
ES
MS
LS
C
ES
B
15
10
5
0
EOGT (TPM)
a
b
a
ES
MS
LS
MS

Figure 3:

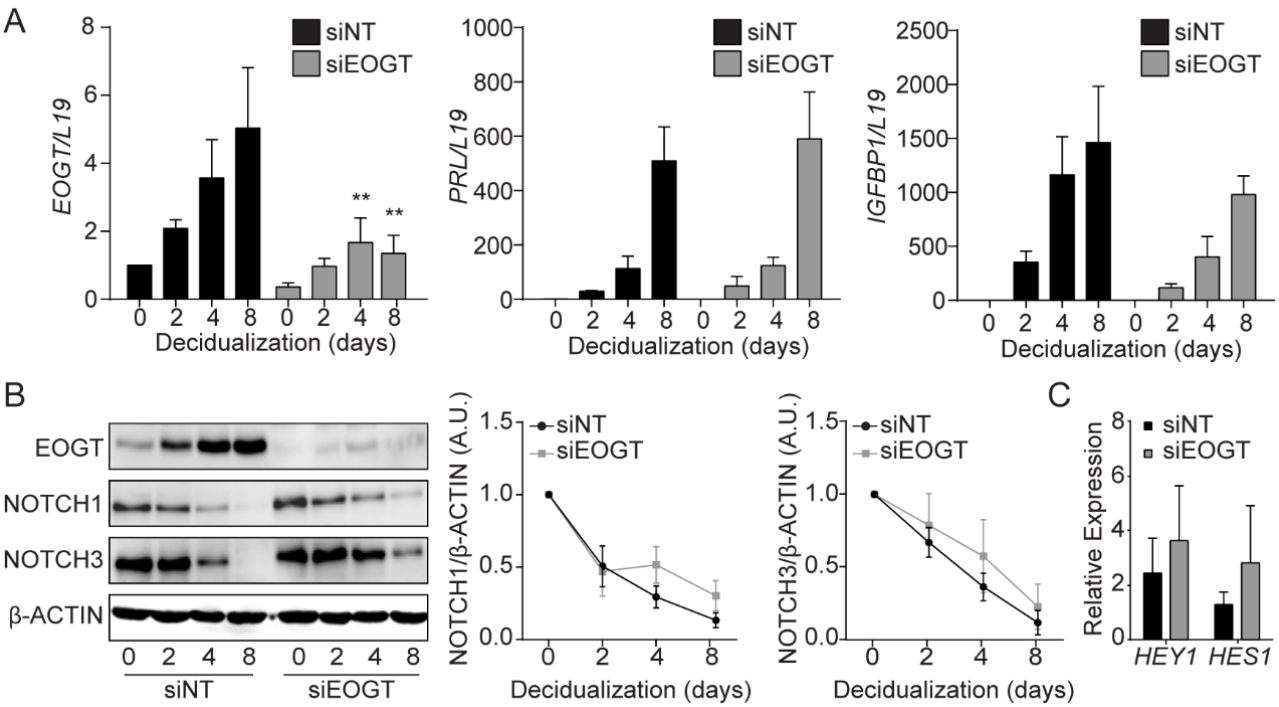
A
siNT
siEOGT
EOGT/L19
PRL/L19
IGFBP1/L19
**
**
Decidualization (days)
B
EOGT
NOTCH1
NOTCH3
β-ACTIN
siNT
siEOGT
NOTCH1/β-ACTIN (A.U.)
NOTCH3/β-ACTIN (A.U.)
C
Relative Expression
HEY1
HES1

Figure 4:

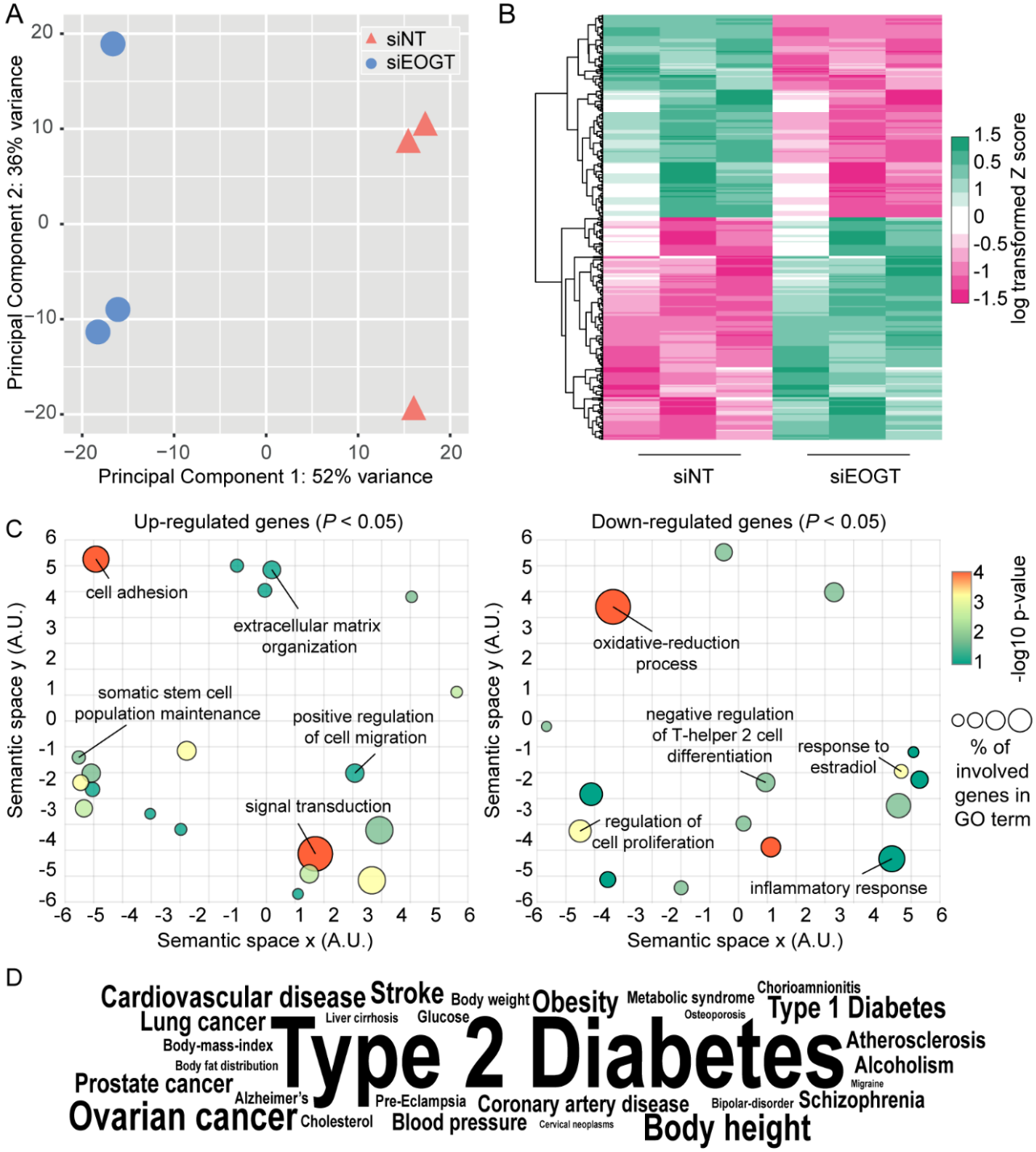
A
siNT
siEOGT
Principal Component 2: 36% variance
Principal Component 1: 52% variance
B
log transformed Z score
siNT
siEOGT
C
Up-regulated genes (P < 0.05)
cell adhesion
extracellular matrix organization
somatic stem cell population maintenance
positive regulation of cell migration
signal transduction
Down-regulated genes (P < 0.05)
oxidative-reduction process
negative regulation of T-helper 2 cell differentiation
response to estradiol
regulation of cell proliferation
inflammatory response
Semantic space x (A.U.)
Semantic space y (A.U.)
-log10 p-value
% of involved genes in GO term
D
Cardiovascular disease
Stroke
Body weight
Obesity
Metabolic syndrome
Osteoporosis
Chorioamnionitis
Type 1 Diabetes
Lung cancer
Liver cirrhosis
Glucose
Body-mass-index
Body fat distribution
Type 2 Diabetes
Atherosclerosis
Alcoholism
Migraine
Prostate cancer
Alzheimer's
Pre-Eclampsia
Coronary artery disease
Bipolar-disorder
Schizophrenia
Ovarian cancer
Cholesterol
Blood pressure
Cervical neoplasms
Body height

Figure 5:

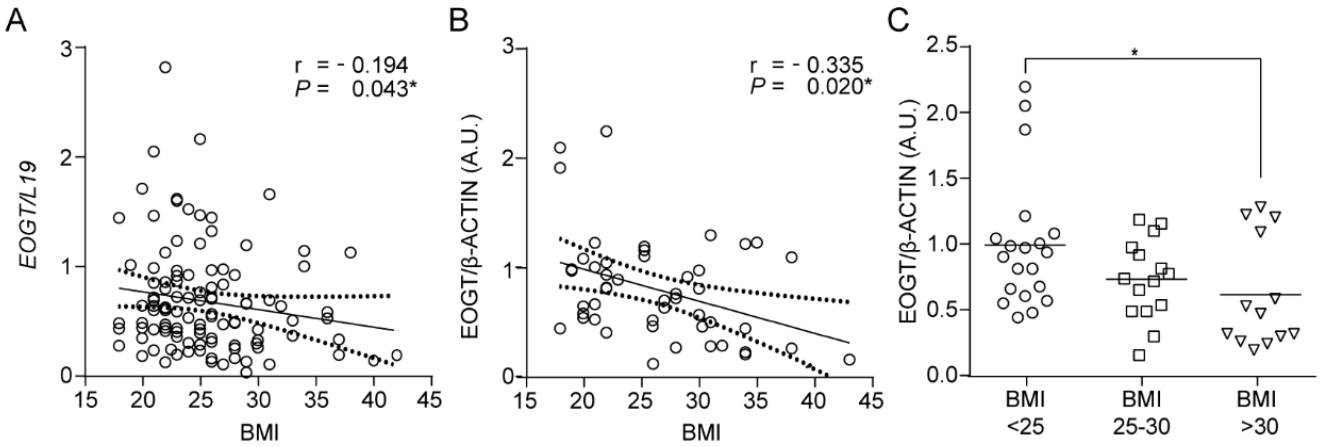
A
r = - 0.194
P = 0.043*
EOGT/L19
BMI
B
r = - 0.335
P = 0.020*
EOGT/β-ACTIN (A.U.)
BMI
C
*
EOGT/β-ACTIN (A.U.)
BMI <25
BMI 25-30
BMI >30

Figure 6:

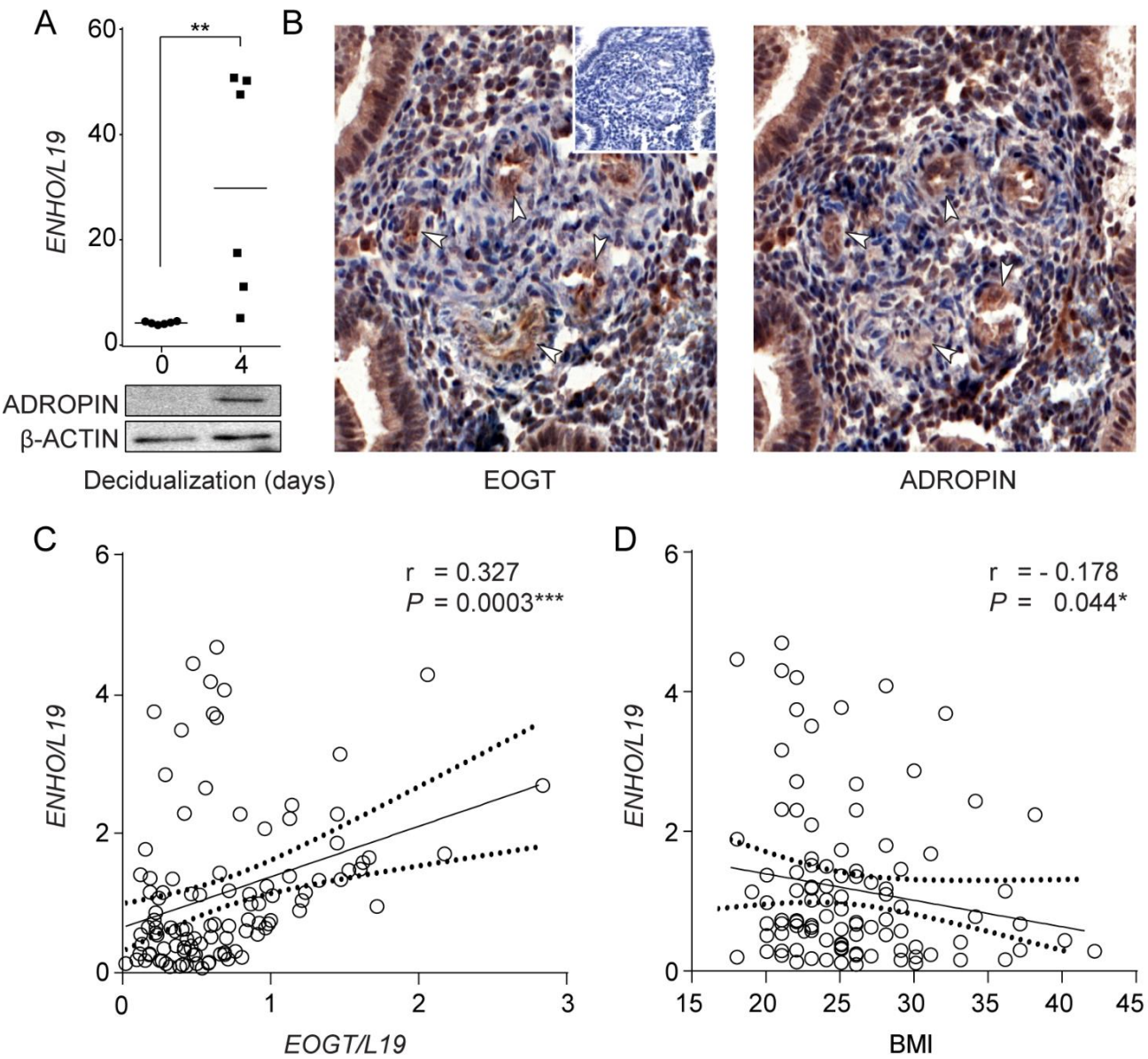
A
B
**
ENHO/L19
60
40
20
0
0
4
ADROPIN
β-ACTIN
Decidualization (days)
EOGT
ADROPIN
C
D
r = 0.327
P = 0.0003***
r = - 0.178
P = 0.044*
ENHO/L19
EOGT/L19
BMI
6
4
2
0
1
2
3
15
20
25
30
35
40
45

THE GLYCOSYLTRANSFERASE EOGT REGULATES ADROPIN EXPRESSION IN DECIDUALIZING HUMAN ENDOMETRIUM – SUPPLEMENTARY FILES

Joanne Muter, Mohammad T Alam, Pavle Vrljicak, Flavio SV Barros, Peter T Ruane, Lauren J Ewington, John D Aplin, Melissa Westwood, and Jan J Brosens.

Supplementary Table 1: Demographic details of 193 participating subjects.

(n=193)	Mean	Standard Deviation
Age (year)	36.1	4.7
Body Mass Index (BMI)	25.9	5.4
First Trimester Loss (n)	3.5	2.3
Day of Cycle (day)	8.0 (Median)	1.5
uNK centile	36.2	25.9

Demographic details of participating subjects in mRNA correlative analysis

(n=112)	Mean	Standard Deviation
Age (year)	35.7	4.8
Body Mass Index (BMI)	25.5	4.9
First Trimester Loss (n)	3.1	2.3
Day of Cycle (day)	8.0 (Median)	1.4
uNK centile	35.8	26.2

Demographic details of participating subjects in protein correlative analysis

(n=48)	Mean	Standard Deviation
Age (year)	36.4	4.4
Body Mass Index (BMI)	26.4	6.0
First Trimester Loss (n)	3.8	2.1
Day of Cycle (day)	8.5 (Median)	1.7
uNK centile	41.2	24.3

Supplementary Table 2: Enriched GO categories upon EOGT knockdown. Categories in *italic* denotes overrepresented GO terms of differentially up-regulated genes. Categories underlined denotes overrepresented GO terms of differentially down-regulated genes.

Category	Term	PValue	%	Count
GO:0007155	*cell adhesion*	*6.93E-05*	*8.57143*	*15*
GO:0007165	*signal transduction*	*2.81E-04*	*13.7143*	*24*
GO:0007411	*axon guidance*	*5.92E-04*	*4.57143*	*8*
GO:0043547	*positive regulation of GTPase activity*	*0.00506*	*7.42857*	*13*
GO:0007605	*sensory perception of sound*	*0.00704*	*3.42857*	*6*
GO:0051056	*regulation of small GTPase mediated signal transduction*	*0.00726*	*3.42857*	*6*
GO:0001822	*kidney development*	*0.00754*	*2.85714*	*5*
GO:0070509	*calcium ion import*	*0.01*	*1.71429*	*3*
GO:0016337	*single organismal cell-cell adhesion*	*0.01309*	*2.85714*	*5*
GO:0045944	*positive regulation of transcription from RNA polymerase II promoter*	*0.01529*	*9.71429*	*17*
GO:0001525	*angiogenesis*	*0.01556*	*4*	*7*
GO:0035235	*ionotropic glutamate receptor signaling pathway*	*0.01948*	*1.71429*	*3*
GO:0035019	*somatic stem cell population maintenance*	*0.02075*	*2.28571*	*4*
GO:0070588	*calcium ion transmembrane transport*	*0.02251*	*2.85714*	*5*
GO:0030335	*positive regulation of cell migration*	*0.02543*	*3.42857*	*6*
GO:0006211	*5-methylcytosine catabolic process*	*0.02674*	*1.14286*	*2*
GO:0007015	*actin filament organization*	*0.02708*	*2.28571*	*4*
GO:0030198	*extracellular matrix organization*	*0.03217*	*3.42857*	*6*
GO:0086091	*regulation of heart rate by cardiac conduction*	*0.03939*	*1.71429*	*3*
GO:0007044	*cell-substrate junction assembly*	*0.04276*	*1.14286*	*2*
GO:0033564	*anterior/posterior axon guidance*	*0.04417*	*1.14286*	*2*
GO:2001199	*negative regulation of dendritic cell differentiation*	*0.04417*	*1.14286*	*2*
GO:0086046	*membrane depolarization during SA node cell action potential*	*0.04417*	*1.14286*	*2*
GO:0030336	*negative regulation of cell migration*	*0.04423*	*2.28571*	*4*
GO:0007517	*muscle organ development*	*0.04623*	*2.28571*	*4*
GO:0055114	oxidation-reduction process	7.06E-05	10.4575	16
GO:0010642	negative regulation of platelet-derived growth factor receptor signaling pathway	0.00127	1.96078	3
GO:0042127	regulation of cell proliferation	0.01593	3.92157	6
GO:0043200	response to amino acid	0.02492	1.96078	3
GO:0042981	regulation of apoptotic process	0.02732	3.92157	6
GO:0006954	inflammatory response	0.0313	5.22876	8
GO:0045629	negative regulation of T-helper 2 cell differentiation	0.03131	1.30719	2
GO:0071395	cellular response to jasmonic acid stimulus	0.03131	1.30719	2
GO:0045920	negative regulation of exocytosis	0.03131	1.30719	2
GO:0030730	sequestering of triglyceride	0.03131	1.30719	2
GO:0043407	negative regulation of MAP kinase activity	0.03291	1.96078	3
GO:0042493	response to drug	0.0341	4.57516	7
GO:0032355	response to estradiol	0.03564	2.61438	4
GO:0042308	negative regulation of protein import into nucleus	0.04152	1.30719	2

GO:0007568	aging	0.04227	3.26797	5
GO:0045627	positive regulation of T-helper 1 cell differentiation	0.0466	1.30719	2
GO:0071799	cellular response to prostaglandin D stimulus	0.0466	1.30719	2

Supplementary Figure 1

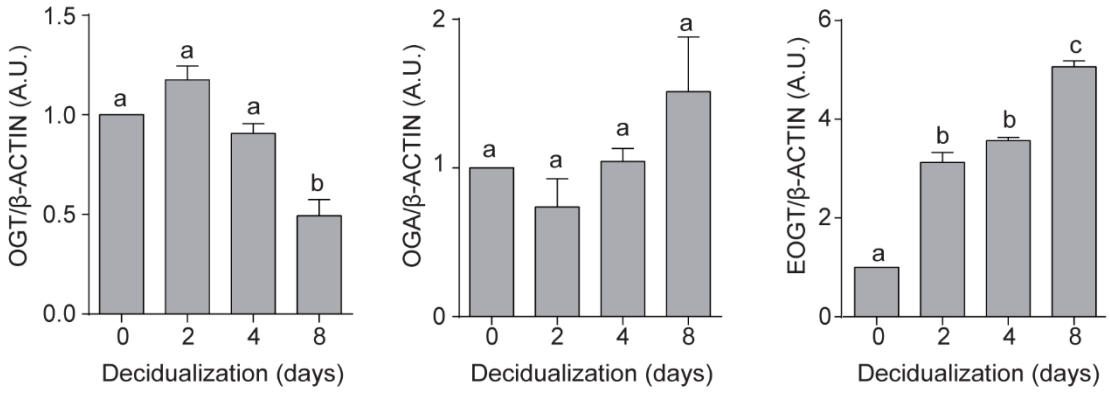

Supplementary Figure 2

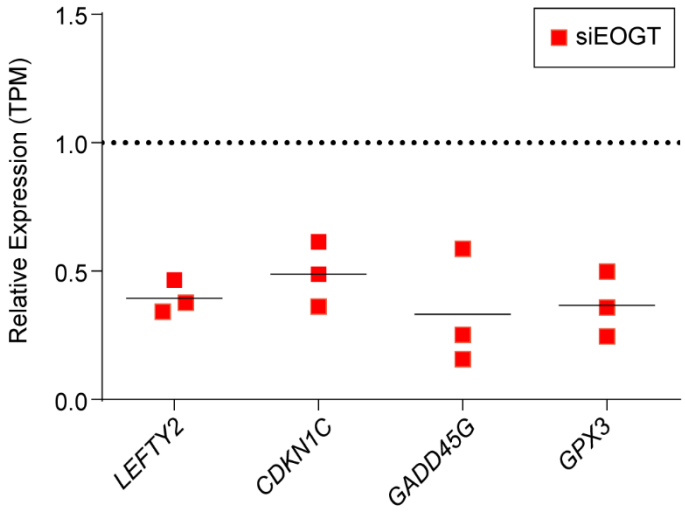

Supplementary Figure 3

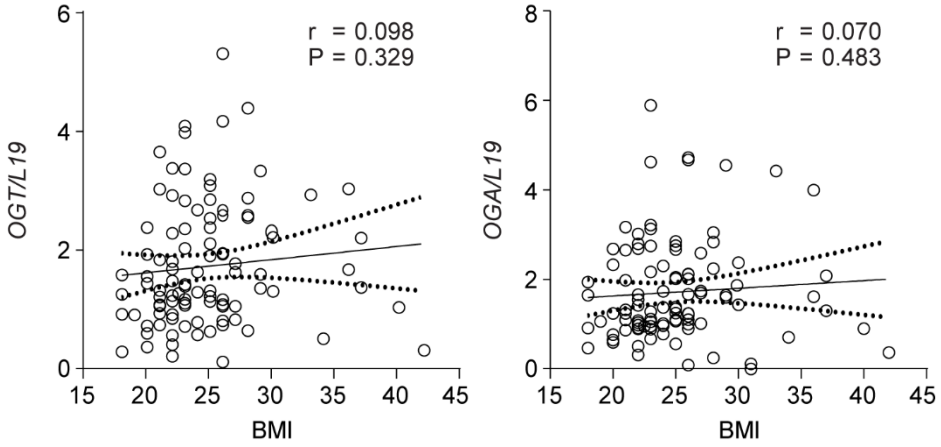

Supplementary Figure 4

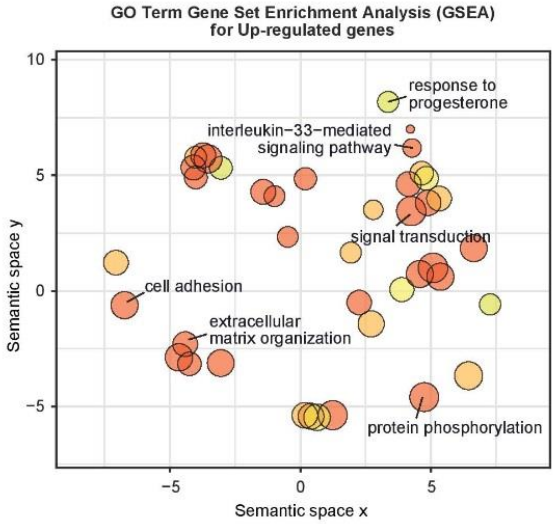

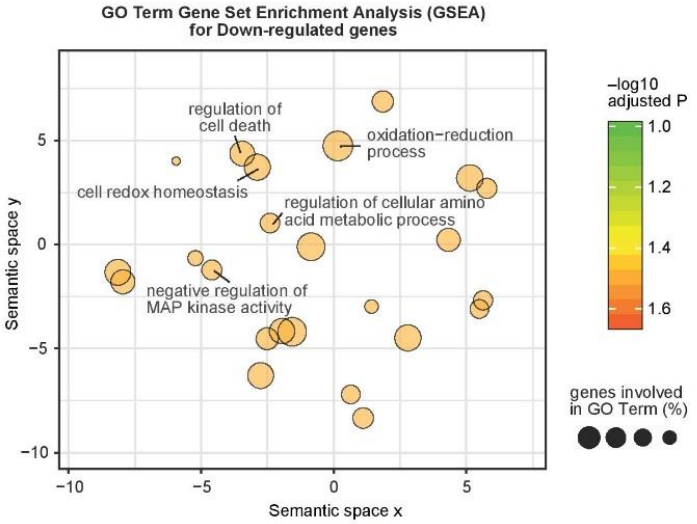

Supplementary Figure 5

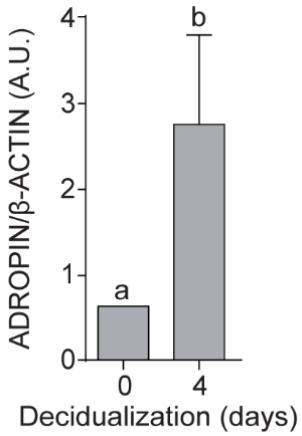

Supplementary Figure 1. *Regulation of O-GlcNAcylation in decidualizing EnSCs. Related to Figure 1.* Densitometric analyses of OGT, OGA and EOGT protein expression from 4 independent primary cultures relative to β-actin expressed as arbitrary units (A.U.). Different letters above the error bars indicate groups are significantly different from each other at $P < 0.05$. Group comparison by ANOVA and post hoc Tukey's test.

Supplementary Figure 2. EOGT *knockdown perturbs distinct gene networks in EnSCs. Related to Figure 4.* Relative expression of *LEFTY2, CDKN1C, GADD45G* and *GPX3* expressed as transcripts per million (TPM) in 3 independent primary EnSC cultures transfected with siEOGT and decidualized for 4 days relative to cultures transfected with siNT (dotted line).

Supplementary Figure 3. EOGT *knockdown perturbs distinct gene networks in EnSCs. Related to Figure 4.* Semantic clustering of significantly overrepresented GO terms ($P < 0.05$) of up- and down-regulated genes (left and right panel, respectively) upon *EOGT* knockdown as ranked by *q* value by GSEA analysis. Circle size is proportional to the percentage of genes in the GO term whereas the color indicates the log10 p-value. Color key is on the right.

Supplementary Figure 4. *Obesity perturbs endometrial EOGT expression. Related to Figure 5.* Pearson's correlation (r) between normalized *OGT* and *OGA* transcript levels in mid-luteal endometrial biopsies and BMI in 112 subjects.

Supplementary Figure 5. *Endometrial ENHO expression relates to BMI. Related to Figure 6.* Densitometric analysis of adropin protein expression from 3 independent primary cultures relative to to β-actin expressed as arbitrary units (A.U.). Different letters above the error bars

indicate groups are significantly different from each other at $P < 0.05$. Group comparison by ANOVA and post hoc Tukey's test.